Photoproduction of π^+ from ^{51}V

Norman Freed
Department of Physics, Pennsylvania State University, University Park, Pennsylvania 16802

Peter Ostrander
Pennsylvania State University, Fayette Campus, Uniontown, Pennsylvania 15401

(Received 10 July 1974)

The reaction $^{51}V(\gamma, \pi^+)^{51}Ti$ is investigated within the impulse approximation. A detailed shell-model calculation is carried out to determine the character of the final nuclear states. We discuss the dependence of the reaction on the single-nucleon production amplitudes, nuclear wave functions, and simulated final state interactions.

[NUCLEAR REACTIONS $^{51}V(\gamma, \pi^+)$ calculated total σ.]

Although 25 years have elapsed since the first experimental studies were carried out on pion photoproduction from free nucleons,[1] it has been only in the past few years that reliable data have been accumulated on the pion photoproduction process on complex nuclei.[2,3] Even though low-energy photoproduction from a single nucleon is well understood in the context of dispersion relations,[4,5] the production process in the nucleus is complicated by many-body effects, the most important of which is pion reabsorption in the final state. Concurrently, the sensitivity of nuclear photoproduction to details of nuclear structure has led to the use of this reaction as a probe of admixtures to nuclear wave functions.[6,7] Interpretation of the data clearly requires a disentanglement of those effects arising from the basic production mechanism from those which are specifically nuclear in origin.

Our aim in this paper is to investigate the extent to which one can understand the photoproduction reaction $^{51}V(\gamma, \pi^+)^{51}Ti$ within the framework of the impulse approximation. We choose this reaction for three reasons. Vanadium is one of a large number of light- and medium-mass nuclei on which photoproduction experiments[3] have recently been carried out with fairly reliable data now available from threshold to 750 MeV. Secondly, the nuclei involved are amenable to shell-model analysis so that the nuclear uncertainties in the problem are greatly minimized. This will enable us to look at the dynamics of the production mechanism relatively unencumbered by questions of nuclear structure. Finally, we want to compare our results with those of a very recent calculation on the same reaction.[8] Since that calculation did not use realistic nuclear wave functions and also employed the older and less reliable CGLN[4] single-nucleon production amplitudes, we will be able to investigate the behavior of the photoproduction cross sections when a better description of the nucleus and more reliable amplitudes[5] are used.

We assume the nuclear photoproduction process to take place via a single-scattering direct reaction mechanism in which the photon makes a single collision with one of the nucleons bound in the nuclear potential well. Although the struck nucleon may change its charge state, we specifically exclude knockout processes and require that the nucleon remain bound. The nonparticipating nucleons are spectators throughout the process to the extent that they do not contribute to optical model elastic scattering of the pion in the exit channel. Although we will discuss the final state interactions later we assume for the moment that they are absent. Thus in the description below the pions are represented by plane waves.

We assume the applicability of the impulse approximation[9] and replace the amplitude for exciting a bound nucleon by the free nucleon amplitude. We may then write for the scattering matrix

$$T_{fi} = \sum_j \langle f | e^{i(\vec{k}-\vec{p})\cdot\vec{r}_j} T_j | i \rangle , \tag{1}$$

where $\vec{k}$ and $\vec{p}$ are the photon and pion momenta and where the pion coordinate $\vec{r}_p$ is evaluated at the location of the jth particle. The matrix elements are taken between the initial and final nuclear states and the sum extends over all nucleons making a transition. T_j is the transition operator for pion photoproduction on a single nucleon and can be written down from conservation principles and invariance requirements in the general form[9]

$$T = (A + \vec{B}\cdot\vec{\sigma})\tau^{(-)} , \tag{2}$$

where $\tau^{(-)}$ is an i-spin operator and where the A

and B are linear combinations of single-nucleon production amplitudes. Averaging over photon polarizations and nuclear spin[10] we find that

$$|T_{fi}|^2=\frac{(4\pi)^2}{2J_i+1}\sum_{n,n'=0,1}\sum_{\lambda=-n}^{n}\sum_{\lambda'=-n'}^{n'}\left[\frac{1}{2}\sum_{\mu=\pm1}F^{n}_{-\lambda}(\mu)F^{n'}_{-\lambda'}(\mu)^*\right]\sum_{K=|J_i-J_f|}^{J_i+J_f}\sum_{ll'L}i^{l-l'}(-)^{K+n+n'+\lambda'}$$

$$\times\left(\frac{(2l+1)(2l'+1)(2L+1)}{4\pi}\right)^{1/2}\begin{pmatrix}L & l & l'\\ 0 & 0 & 0\end{pmatrix}\begin{pmatrix}L & n' & n\\ \lambda'-\lambda & -\lambda' & \lambda\end{pmatrix}\begin{Bmatrix}L & n' & n\\ K & l & l'\end{Bmatrix}Y_L^{\lambda-\lambda'}(\hat{q})$$

$$\times\langle J_f||\sum_j j_l(qr_j)S_{lnk}(j)||J_i\rangle\langle J_f||\sum_j j_{l'}(qr_j)S_{l'n'K}(j)||J_i\rangle^*. \tag{3}$$

Here J_i and J_f are the initial and final nuclear spins and $\vec{q}=\vec{k}-\vec{p}$ is the momentum transfer to the nucleus. The $Y_L(\hat{q})$ and $j_l(qr)$ are the usual spherical harmonic and spherical Bessel functions and the S_{lnK} is the tensor product $[Y_l(\hat{r})\otimes\sigma_n]^K$ with $\sigma_0=1$ and $\sigma_1=\vec{\sigma}$. The bracketed expression[10] involves only the single-nucleon amplitudes and is calculated using the multipole analysis of Berends, Donnachie, and Weaver.[5] We retain the multipoles E_{0^+}, E_{1^+}, E_{2^-}, M_{1^+}, and M_{1^-} although the E_{0^+} and M_{1^+} give by far the dominant contributions.

The nuclear features of the process are contained in the reduced matrix elements. We assume an inert ^{48}Ca core and write the ^{51}V ground state wave function $|J_i\rangle=|(1f_{7/2p})^3;\ \frac{7}{2}^-\rangle$. Since the experimental cross sections are deduced from β-decay activation measurements,[3] only those low-lying states in ^{51}Ti which are bound against nucleon emission will contribute. The sum in the reduced matrix element will therefore include only valence nucleons since core-excited configurations will correspond to energies greater than neutron threshold at 6.38 MeV. With this in mind, we have performed a shell-model calculation on ^{51}Ti retaining all 36 states occurring below threshold. The basic configurations are all of the form $|(1f_{7/2p})^2(J),j_n;J_f\rangle$ where the allowed neutron states j_n are $2p_{3/2}$, $2p_{1/2}$, $1f_{5/2}$, and $1g_{9/2}$. The neutron single-particle energies and proton-proton matrix elements are taken from the experimental spectra of ^{49}Ca and ^{50}Ti and the neutron-proton elements from recent shell-model calculations in the $N=28$ region.[11] If we then write $|J_f\rangle=\sum_{j_nJ}b(j_nJJ_f)|(f_{7/2})^2(J),j_n;J_f\rangle$, where the b's result from our shell-model calculation, we find

$$\langle J_f||\sum_j j_l(qr_j)S_{lnK}(j)||J_i\rangle=(-)^{J_f+K-1/2}[24(2J_f+1)]^{1/2}$$

$$\times\sum_{j_nJ}a(J)b(j_nJJ_f)\begin{Bmatrix}j_n & J_f & J\\ \frac{7}{2} & \frac{7}{2} & K\end{Bmatrix}\langle j_n||j_l(qr)S_{lnK}||f_{7/2}\rangle. \tag{4}$$

The $a(J)$ are the fractional parentage coefficients arising from the antisymmetrization of $(f_{7/2})^3$. The single-particle reduced matrix element is found to be

$$\langle j_n||j_l(qr)S_{lnK}||f_{7/2}\rangle=(-)^{l_n}\left(\frac{56(2j_n+1)(2l_n+1)(2l+1)(2K+1)(4n+2)}{4\pi}\right)^{1/2}\begin{Bmatrix}l_n & \frac{1}{2} & j_n\\ 3 & \frac{1}{2} & \frac{7}{2}\\ l & n & K\end{Bmatrix}\begin{pmatrix}l_n & l & 3\\ 0 & 0 & 0\end{pmatrix}$$

$$\times\int_0^\infty R^*_{n_n l_n}(r)j_l(qr)R_{1f}(r)r^2dr, \tag{5}$$

in terms of the harmonic oscillator wave functions $R_{nl}(r)$. We take the oscillator length $b=2.03$ fm consistent with electron scattering data. Finally, the total cross sections are calculated from

$$\sigma=(2\pi)^4\int d\vec{p}\,\delta(k-E_f-q^2/2M_f-(p^2+\mu^2)^{1/2})\,|T_{fi}|^2, \tag{6}$$

where μ is the pion mass, E_f is the excitation energy of the residual nucleus, and M_f is its mass. All quantities are in the lab system except for the single-nucleon amplitudes in $|T_{fi}|^2$. Converting the amplitudes from the pion-nucleon c.m. to the lab introduces into $|T|^2$ an additional q dependence.

Until now we have neglected the fact that the pion wave function is distorted by the presence

of the Coulomb and nuclear potentials. The assumption of plane wave pions enabled us to calculate the cross section analytically in terms of the momentum transfer to the nucleus. If we replace $e^{-i\vec{p}\cdot\vec{r}}$ in Eq. (1) by a wave function describing the scattering state of the pion-nucleus system, we can no longer carry out the sum over all partial waves analytically and must resort to a numerical solution of the Klein-Gordon equation in order to generate the appropriate optical-model wave functions.[12] Although such a program is now underway, the problem is made considerably more complicated. In order to get a qualitative idea of the importance of final state effects, we utilize here the so-called surface production model.[6,13] This model, in which pions are produced on the nuclear surface, is designed to simulate the strong pion absorption in the (3, 3) resonance region through a cutoff, r_0 (usually taken to be the nuclear radius), in the lower limit of the overlap integral appearing in Eq. (5). Since our model involves production only from valence nucleons, we expect to achieve at least a reasonable estimate of the effect of using distorted waves for the pion.

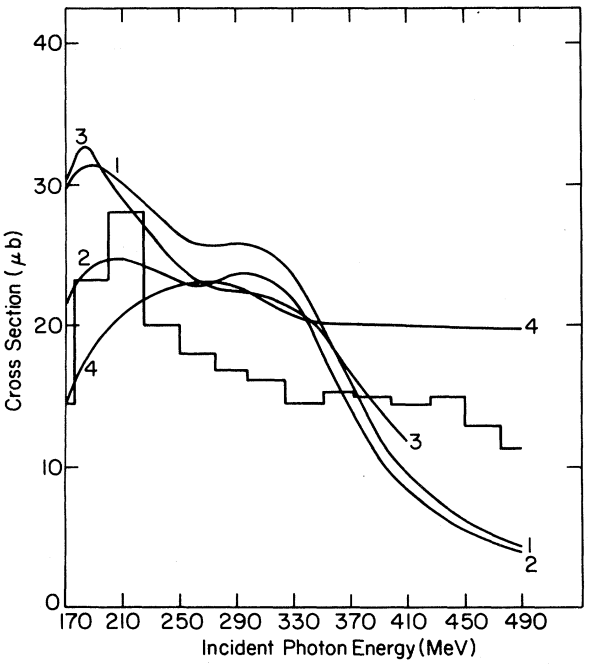

FIG. 1. Cross sections for the reaction $^{51}V(\gamma,\pi^+)^{51}Ti$. Curve 1: results of present calculation using Berends amplitudes, shell-model wave functions and no final state interactions; curve 2: same as curve 1 with simulated final state interactions; curve 3: results of Ref. 8 with CGLN amplitudes, simplified shell-model wave functions and simulated final state interactions; curve 4 and the histogram: experimental results of Refs. 3(a) and 3(b), respectively. See text for details.

Our results are summarized in Fig. 1. We have plotted cross sections calculated with and without simulated final state interactions and have included for comparison the theoretical predictions of Ref. 8 and experiment (Ref. 3). We note first that the curves are reminiscent of those for the single nucleon production process[14] with the nuclear kinematics reducing in size and shifting the (3, 3) resonance peak. It is also worth mentioning that at low energies the cross sections utilizing configuration mixed wave functions are approximately 3 times greater than those for which the final states in ^{51}Ti are assumed to be the pure neutron configurations $p_{3/2}$, $p_{1/2}$, $f_{5/2}$, and $g_{9/2}$. As one illustration of the effect of higher-seniority components, we find that near threshold the pure $v=3$ $\frac{7}{2}^-$ and $\frac{9}{2}^-$ states (10 in total) contribute approximately $\frac{1}{4}$ of the cross section. Approximately half the cross section comes from the aggregate of $\frac{5}{2}^-$ and $\frac{9}{2}^+$ states. Our shell-model calculation indicates that the $f_{5/2}$ single-neutron strength is considerably fractionated, none of the six $\frac{5}{2}^-$ states below 6.4 MeV containing more than 40% of the total strength. Roughly half the contribution of the $\frac{5}{2}^-$ states to the cross section comes from one level, calculated at 5.39 MeV, which contains significant admixtures of the configurations $|f_{7/2}^2(0)f_{5/2}\rangle$, $|f_{7/2}^2(2)p_{1/2}\rangle$, $|f_{7/2}^2(2)f_{5/2}\rangle$, and $|f_{7/2}^2(4)f_{5/2}\rangle$. In view of the fact that the nuclear matrix elements for pion photoproduction are formally identical to those for β decay, it is interesting to note that the cross section for the single-particle transition $f_{7/2}\rightarrow f_{5/2}$ is smaller than that for $f_{7/2}\rightarrow g_{9/2}$. Although the β decays are allowed and first forbidden, respectively, the kinematics has an overriding effect, favoring non-spin-flip over non-parity-change processes.

A comparison of curves 1 and 2 illustrates the effect of final state interactions. Although our treatment is necessarily qualitative, we find an over-all reduction of the cross section by approximately 25% near threshold. This is consistent with the results of a recent threshold calculation[15] on $^{12}C(\gamma,\pi^+)^{12}B$ in which the full nuclear potential was allowed to distort s-wave pions (cf. also Ref. 16). The cutoff used in the calculation for curve 2 was chosen to be $r_0=3.68$ fm, corresponding to the rms nuclear radius. We find that the results are quite sensitive to the precise value of r_0. For example, increasing r_0 by 10% results in an additional 15% reduction in the cross section near threshold. Such sensitivity implies that agreement with experiment for a particular value of r_0 may be fortuitous. Furthermore, we find that the effects of varying r_0 can often be simulated by varying other parameters of the problem (e.g., by altering the treatment of the

nuclear states). This implies a certain degree of arbitrariness in identifying the cutoff parameter as the nuclear radius. We conclude that although the surface production mechanism may provide a rough estimate of the relative importance of final state interactions, its connection to the fundamental pion distortion and absorption processes is not sufficiently clear to allow detailed conclusions to be drawn from comparison with experiment.

Apart from effects which we calculate to be small, curves 2 and 3 differ in the choice of single nucleon amplitudes and in the treatment of the final nuclear states. The results of Ref. 8 were based on the CGLN amplitudes[4] with Roper phase shifts, while ours are based on the more accurate multipole analysis of Berends, Donnachie, and Weaver.[5] In Ref. 8 all of the strength corresponding to the single nucleon transitions $f_{7/2} \rightarrow f_{5/2}$, $g_{9/2}$, $p_{3/2}$, and $p_{1/2}$ was included in the calculation of the cross sections. In our shell-model treatment we find that much of this strength (particularly for the transitions $f_{7/2} \rightarrow f_{5/2}$ and $f_{7/2} \rightarrow g_{9/2}$) resides in unbound states of the final system and will therefore not contribute to cross sections measured by activation analysis. The relative flattening (curve 2 vs 3) of the cross section from threshold to the (3, 3) resonance arises from the smaller Berends electric dipole amplitudes. This leads to strong interference between the s- and p-wave contributions which peak roughly at 200 and 300 MeV. This effect, most pronounced for the dominant $f_{7/2} \rightarrow f_{5/2}$ and $f_{7/2} \rightarrow g_{9/2}$ transitions, results in a broadening of the peaks corresponding to the individual contributions.

The experimental results are shown in curve 4[3(a)] and on the histogram,[3(b)] the latter arising from application of a scale factor to the ^{27}Al(γ, π^+)-^{27}Mg cross section. Although, as we have indicated, detailed comparisons are premature, we find that our primary result (curve 2) is reasonably consistent with experiment from threshold to 400 MeV. Our calculated results tend to drop too rapidly in the range 400–500 MeV and are therefore somewhat lower than experiment at higher energies [data are available[3] up to $E_\gamma = 750$ MeV, the energy of the $N(1525)$ resonance].

To conclude, we have applied the impulse approximation to the pion photoproduction process using the most accurately determined single-nucleon production amplitudes and employing a detailed description of the final nuclear states. The effect of pion reabsorption in the final state has been taken into account qualitatively. We have not discussed the possible influence of nuclear Fermi motion, two-pion production, ground state correlations in ^{51}V, and particle-hole states[17] in ^{51}Ti but have estimated these effects to be small at photon energies less than 400 MeV. We have assumed the T_j to vary slowly off the energy shell, an approximation which should be reasonably valid except near the (3, 3) resonance. Although our calculations were confined to the reaction ^{51}V-$(\gamma, \pi^+)^{51}$Ti, we have also investigated positive pion production on ^{27}Al and negative pion production from ^{11}B with similar results. Detailed comparison with experiment must await a more careful treatment of final state effects.[18]

One of us (N.F.) would like to acknowledge the kind hospitality of Professor R. Piepenbring and the Institut des Sciences Nucléaires of the Université de Grenoble, where this work was begun.

[1] J. Steinberger and A. S. Bishop, Phys. Rev. 78, 493 (1950).
[2] W. B. Walters and J. P. Hummel, Phys. Rev. 143, 833 (1966).
[3] (a) G. Nydahl and B. Forkman, Nucl. Phys. B7, 97 (1968); (b) I. Blomqvist, G. Nydahl, and B. Forkman, Nucl. Phys. A162, 193 (1971).
[4] G. F. Chew, M. L. Goldberger, F. E. Low, and Y. Nambu, Phys. Rev. 106, 1337, 1345 (1957).
[5] F. A. Berends, A. Donnachie, and D. L. Weaver, Nucl. Phys. B4, 54, 103 (1967).
[6] V. Devanathan, M. Rho, K. Rao, and S. Nair, Nucl. Phys. B2, 329 (1967); K. Rao and V. Devanathan, Phys. Lett. 32B, 578 (1970).
[7] A. K. Rej and T. Engeland, Phys. Lett. 45B, 77 (1973).
[8] V. Devanathan, G. Prasad, and K. Rao, Phys. Rev. C 8, 188 (1973).
[9] M. L. Goldberger and K. M. Watson, *Collision Theory* (Wiley, New York, 1964).
[10] L. M. Saunders, Nucl. Phys. B7, 293 (1968).
[11] J. Vervier, Nucl. Phys. 78, 497 (1966); H. Horie and K. Ogawa, Prog. Theor. Phys. 46, 439 (1971).
[12] E. H. Auerbach, D. M. Fleming, and M. M. Sternheim, Phys. Rev. 162, 1683 (1967).
[13] E. W. Laing and R. G. Moorhouse, Proc. Phys. Soc. Lond. A70, 629 (1952).
[14] G. Källén, *Elementary Particle Physics* (Addison-Wesley, Reading, 1964).
[15] J. H. Koch and T. W. Donnelly, Nucl. Phys. B64, 478 (1973).
[16] J. B. Seaborn, V. Devanathan, and H. Überall, Nucl. Phys. A219, 461 (1974); E. Borie, H. Chandra, and D. Drechsel, *ibid.* A226, 58 (1974).
[17] R. N. Glover, A. Denning, and G. Brown, Phys. Lett. 27B, 434 (1968).
[18] N. Freed and P. Ostrander, unpublished.